



# Crystal structure and Hirshfeld surface analysis of a pyridinium bromide salt: 1-[2-(adamantan-1-yl)-2-oxoethyl]pyridin-4-iminium bromide

Huey Chong Kwong,<sup>a</sup> Imdad Mahmud Pathi,<sup>b</sup> C. S. Chidan Kumar,<sup>c\*</sup> Ching Kheng Quah<sup>b</sup> and Md. Azharul Arafath<sup>d\*</sup>

Received 4 June 2018

Accepted 25 June 2018

Edited by C. Rizzoli, Università degli Studi di Parma, Italy

**Keywords:** crystal structure; pyridinium salt; hydrogen bonding; Hirshfeld surface analysis.

**CCDC reference:** 1851334

**Supporting information:** this article has supporting information at journals.iucr.org/e

<sup>a</sup>School of Chemical Sciences, Universiti Sains Malaysia, 11800 USM, Penang, <sup>b</sup>X-ray Crystallography Unit, School of Physics, Universiti Sains Malaysia, 11800 USM, Penang, Malaysia, <sup>c</sup>Department of Engineering Chemistry, Vidya Vikas Institute of Engineering & Technology, Visvesvaraya Technological University, Alanahalli, Mysuru 570028, Karnataka, India, and <sup>d</sup>Department of Chemistry, Shahjalal University of Science and Technology, Sylhet 3114, Bangladesh.

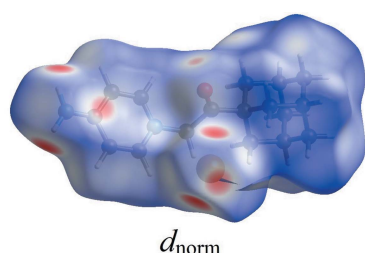
\*Correspondence e-mail: chidankumar@gmail.com, arafath\_sustche90@yahoo.com

In the cation of the title salt,  $C_{17}H_{23}N_2O^+ \cdot Br^-$ , the adamantyl moiety and the pyridinium ring are inclined to the ketone bridge by torsion angles of  $-78.1(2)^\circ$  ( $C-C-C=O$ ) and  $58.3(2)^\circ$  ( $C-C-N-C$ ), respectively, and the ketone bridge has a  $C-C-C-N$  torsion angle of  $174.80(15)^\circ$ . In the crystal, the cations are connected into chains parallel to the  $c$  axis by  $C-H \cdots O$  hydrogen bonds. The chains are further linked into layers parallel to the  $bc$  plane by  $N-H \cdots Br$  and  $C-H \cdots Br$  hydrogen bonds,  $C-H \cdots \pi$  interactions and  $\pi-\pi$  stacking interactions [centroid-to-centroid distance =  $3.5657(11) \text{ \AA}$ ]. A Hirshfeld surface analysis, which comprises the  $d_{norm}$  surface, electrostatic potential map and two-dimensional fingerprint plots, was carried out to verify the contribution of the various intermolecular interactions.

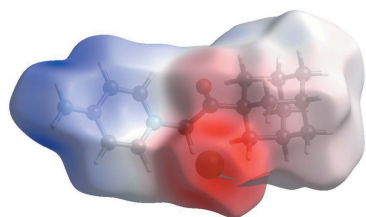
## 1. Chemical context

Adamantane derivatives have been shown to exhibit various biological activities such as antiviral (Zoidis *et al.*, 2010), anti-diabetic (Zettl *et al.*, 2010), antimicrobial (Piérard *et al.*, 2009), anti-inflammatory (Lamanna *et al.*, 2012), antioxidant (Priyanka *et al.*, 2013) and central nervous system activities (Reisberg *et al.*, 2003). Besides, adamantane-based chemotherapeutics have been developed for treating viral infections, for example influenza A, herpes simplex and HIV (Liu *et al.*, 2011). There are a number of negatively charged enzymes and cofactors and many diseases, including cystic fibrosis, have been found to result from defects in the ion channel function (Ashcroft, 1999). The anion- $\pi$  non-covalent interaction has been explored both theoretically and experimentally and selective anion receptors and channels have been designed (Ballester, 2008; Schottel *et al.*, 2008; Hay & Bryantsev, 2008; Frontera *et al.*, 2011).

Ionic liquids (ILs) have attracted a lot of interest over the past decade because of their unusual range of properties such as negligible vapour pressure, excellent thermal stability in a wide temperature range, no flammability and high ionic conductivity (Davis, 2004). ILs are excellent alternatives to volatile organic compounds (VOCs). An ionic liquid has a strong solvation ability and can dissolve polar and non-polar species with efficient selectivity, which can be modified by

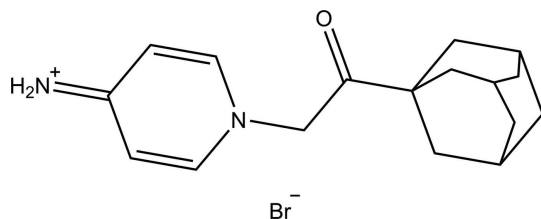


$d_{norm}$



Electrostatic Potential

changing the anion (Blanchard *et al.*, 2001). ILs have been used successfully as solvents in several reactions such as isomerization, dimerization, hydrogenation, and Heck and Suzuki coupling reactions (Chauvin & Olivier-Bourbigou, 1995; Holbrey & Seddon, 1999). They have also performed well as solvents in bio-catalysed and homogeneous catalytic reactions, and can be used as lubricants to wet the surface of metals, polymers and inorganic materials (Crosthwaite *et al.*, 2004).



## 2. Structural commentary

Fig. 1 shows the asymmetric unit of the title salt, which consists of a 1-[2-(adamantan-1-yl)-2-oxoethyl]pyridin-4-iminium cation and a bromide anion. The cation is constructed from an adamantyl moiety (C1–C10) and a pyridinium ring (N1/C13–C17), which are connected by a ketone bridge [(C11=O1)–C12]. The bond angles formed by the quaternary carbon (C1) with the surrounding secondary carbons (C2, C6 and C7) are comparable with those reported for related structures which range from 107.40 (12) to 110.82 (13)° (Rouchal *et al.*, 2011). Both the adamantyl and pyridinium rings are twisted away from the ketone bridge to reduce repulsion, as indicated by the torsion angles C6–C1–C11=O1 [–78.1 (2)°] and C11–C12–N1–C13 [58.3 (2)°]. The ketone bridge is in an *antiperiplanar* conformation [C1–C11–C12–N1 = 174.80 (15)°]. The dihedral angle formed by the pyridinium ring with the ketone bridge is 59.77 (14)°. Bond lengths and angles in the cation are within normal ranges (Allen, 2002). However, the N2–C15 bond length [1.325 (2) Å] is shorter than expected for an NH<sub>2</sub>–C<sub>ar</sub> single bond [1.38 (3) Å], indicating partial double-bond character. Similar bond lengths are found in related compounds with an N<sup>+</sup>=C double bond (Chidan Kumar *et al.*, 2017; Sharmila *et al.*, 2014; Yue *et al.*, 2013).

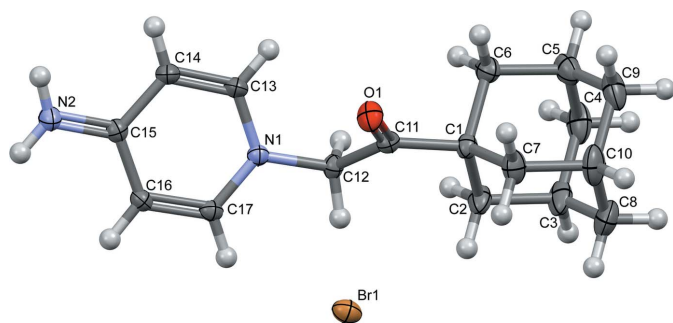


**Figure 1**

The molecular structure of the title salt with displacement ellipsoids drawn at the 50% probability level.

**Table 1**

Hydrogen-bond geometry (Å, °).

Cg1 is the centroid of the N1/C13–C17 ring.

<i>D</i> –H... <i>A</i>	<i>D</i> –H	H... <i>A</i>	<i>D</i> ... <i>A</i>	<i>D</i> –H... <i>A</i>
N2–H1N2...Br1 <sup>i</sup>	0.84 (2)	2.73 (2)	3.499 (2)	153 (2)
N2–H2N2...Br1 <sup>ii</sup>	0.85 (2)	2.56 (2)	3.393 (2)	169 (2)
C12–H12A...Br1 <sup>iii</sup>	0.97	2.72	3.664 (2)	166
C17–H17A...O1 <sup>iv</sup>	0.93	2.59	3.434 (2)	150
C14–H14A...Cg1 <sup>i</sup>	0.93	2.94	3.608 (2)	130

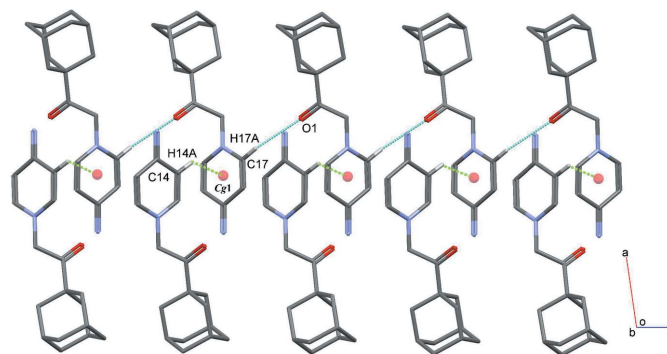
Symmetry codes: (i)  $-x, y - \frac{1}{2}, -z + \frac{1}{2}$ ; (ii)  $-x, -y + 1, -z + 1$ ; (iii)  $x, y - 1, z$ ; (iv)  $x, -y + \frac{1}{2}, z + \frac{1}{2}$ .

## 3. Supramolecular features

In the crystal, the cations are linked into chains along the *c*-axis direction *via* C17–H17A...O1 hydrogen bonds (Table 1, Fig. 2). The chains interact through N–H...Br and C–H...Br hydrogen bonds to form layers parallel to the *bc* plane, which are further enforced by C–H... $\pi$  and  $\pi$ – $\pi$  interactions [centroid-to-centroid distance 3.5657 (11) Å].

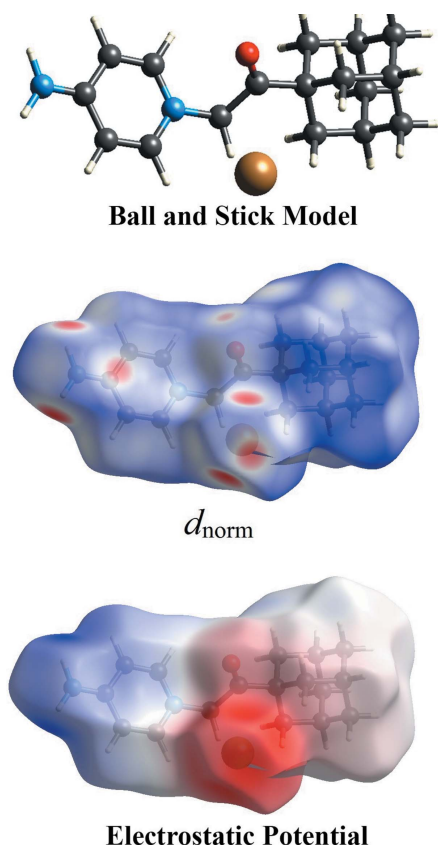
## 4. Hirshfeld Surface Analysis

The Hirshfeld surface analysis (Spackman & Jayatilaka, 2009) of the title salt was performed using *CrystalExplorer3.1* (Wolff *et al.*, 2012), and comprises  $d_{\text{norm}}$  surface plots, electrostatic potentials and two-dimensional fingerprint plots (Spackman & McKinnon, 2002). The ball-and-stick model,  $d_{\text{norm}}$  surface and electrostatic potential plots of the title salt are shown in Fig. 3. Those plots were generated in order to quantify and give visual confirmation of the intermolecular interactions and to explain the observed crystal packing. The dark-red spots on the  $d_{\text{norm}}$  surface arise because of short interatomic contacts, while the other weak intermolecular interactions appear as light-red spots. Furthermore, the negative electrostatic potential (red region) in the electrostatic potential map indicates hydrogen-acceptor potential, whereas the hydrogen donors are represented by positive electrostatic potential (blue region) (Spackman *et al.*, 2008).



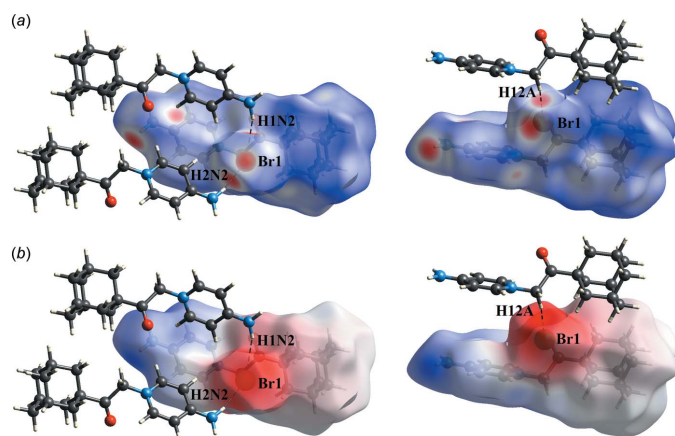
**Figure 2**

Partial packing diagram of the the cations showing the C17–H17A...O1 hydrogen bonds (blue dashed lines) and the C14–H14A... $\pi$  interactions (green dashed lines).

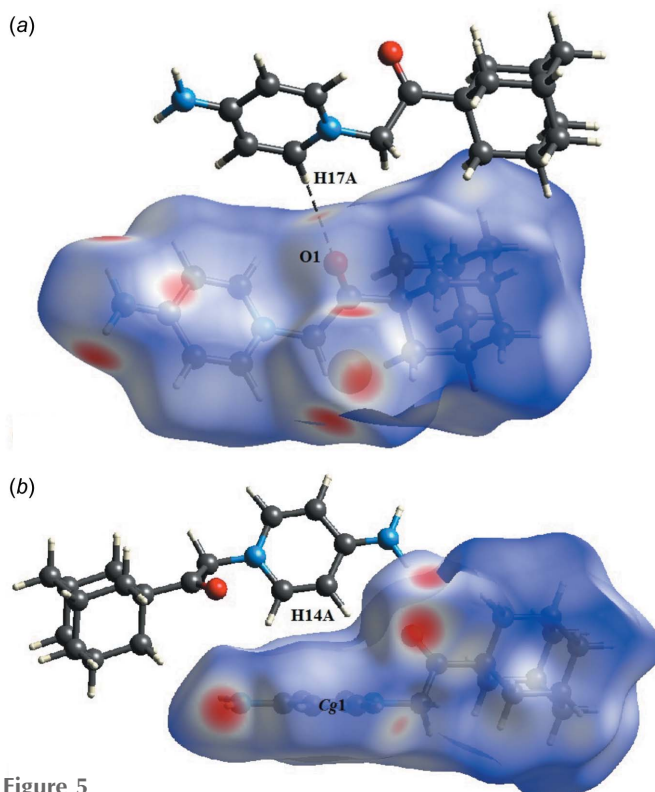

**Figure 3**

Hirshfeld surfaces mapped over  $d_{\text{norm}}$  and electrostatic potential to visualize the intermolecular contacts in the title salt. The molecule in the ball-and-stick model is in the same orientation shown in the Hirshfeld surface and electrostatic potential plots.

Dark-red spots that are close to atoms H1N2, H2N2, H12A and Br1 in the  $d_{\text{norm}}$  surface mapping are the result of the N2—H1N2···Br1, N2—H2N2···Br1 and C12—H12A···Br1 hydrogen bonds (Fig. 4a). This observation is further confirmed by the respective electrostatic potential maps where Br1 shows negative electrostatic potential as a hydrogen


**Figure 4**

A visualization of the N—H···Br and C—H···Br interactions. (a)  $d_{\text{norm}}$  and (b) electrostatic potential mapped on Hirshfeld surfaces in order to visualize the N—H···Br and C—H···Br interactions (black dotted lines).


**Figure 5**

$d_{\text{norm}}$  mapped on Hirshfeld surfaces in order to visualize (a) the C—H···Br hydrogen bond (black dashed line) and (b) the C—H··· $\pi$  interactions.

acceptor (red region, Fig. 4b). Besides those two short intermolecular contacts, the C—H···O and C—H··· $\pi$  interactions are shown as light-red spots on the  $d_{\text{norm}}$  surface (Fig. 5).

A quantitative analysis of the intermolecular interactions can be made by studying the fingerprint plots (FP); characteristic pseudo-symmetry wings in the  $d_e$  and  $d_i$  diagonal axes can be seen in the overall two-dimensional FP (Fig. 6). The most significant intermolecular interactions are the H···H interactions (63.5%), which appear in the central region of the FP with  $d_e = d_i \approx 2.2$  Å (Fig. 6b). The reciprocal H···Br/Br···H and H···O/O···H interactions with 15.9% and 7.6% contributions, respectively are present as sharp symmetrical spikes at  $d_e + d_i \approx 2.4$  and 2.5 Å, respectively (Fig. 6c and 6e). The reciprocal H···C/C···H interactions appear as two symmetrical narrow wings at  $d_e + d_i \approx 2.5$  Å and contribute 7.8% to the Hirshfeld surface (Fig. 6d). The reciprocal N···H/H···N interactions appear as a symmetrical V-shaped wing in the FP map with  $d_e + d_i \approx 2.7$  Å and contribute 2.7% to the Hirshfeld surface (Fig. 6f). The percentage contributions for other intermolecular contacts are less than 2.6%.

## 5. Synthesis and crystallization

A mixture of 1-adamantly bromomethyl ketone (2.75 g, 10 mmol) and 4-aminopyridine (0.11 g, 1 mmol) was dissolved in 10 ml of toluene at room temperature, followed by stirring at 358 K for 18 h. The completion of the reaction was marked by the amount of the separated solid from the initially clear

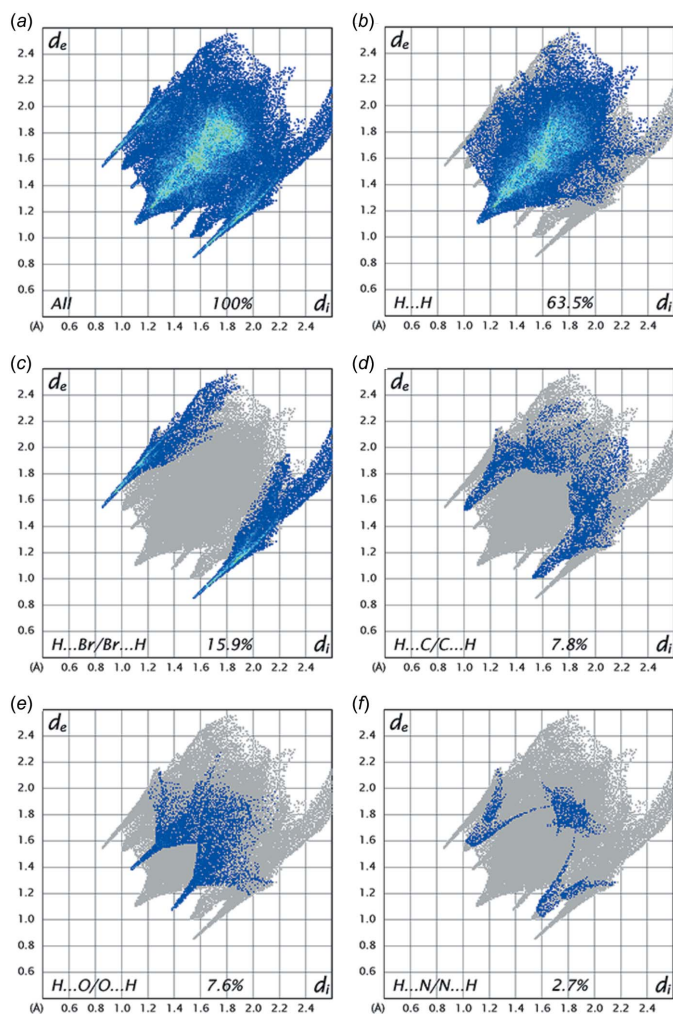


Figure 6  
Fingerprint plots.

and homogeneous mixture of the starting materials. The solid was filtered and washed by ethyl acetate. The final pyridinium salt was obtained after the solid had been dried under reduced pressure to remove all volatile organic compounds (Said *et al.*, 2017; Sheshadri *et al.*, 2018). Plate-like colourless crystals were obtained by slow evaporation of an acetone solution.

## 6. Refinement

Crystal data, data collection and structure refinement details are summarized in Table 2. C-bound H atoms were positioned geometrically [ $C-H = 0.93-0.98 \text{ \AA}$ ] and refined using a riding model with  $U_{\text{iso}}(\text{H}) = 1.2U_{\text{eq}}(\text{C})$ . The N-bound H atoms were located in a difference-Fourier map and freely refined. One outlier (100) was omitted in the last cycles of refinement.

## Funding information

HCK thanks the Malaysian Government for a MyBrain15 scholarship.

Table 2

Experimental details.

Crystal data	
Chemical formula	$C_{17}H_{23}N_2O^+ \cdot Br^-$
$M_r$	351.28
Crystal system, space group	Monoclinic, $P2_1/c$
Temperature (K)	294
$a, b, c$ (Å)	18.758 (2), 7.1508 (8), 11.9909 (14)
$\beta$ (°)	98.2117 (17)
$V$ (Å <sup>3</sup> )	1591.9 (3)
$Z$	4
Radiation type	Mo $K\alpha$
$\mu$ (mm <sup>-1</sup> )	2.58
Crystal size (mm)	$0.38 \times 0.25 \times 0.09$
Data collection	
Diffractometer	Bruker APEXII DUO CCD area-detector
Absorption correction	Multi-scan (SADABS; Bruker, 2012)
$T_{\text{min}}, T_{\text{max}}$	0.320, 0.408
No. of measured, independent and observed [ $I > 2\sigma(I)$ ] reflections	35418, 4897, 3392
$R_{\text{int}}$	0.051
$(\sin \theta/\lambda)_{\text{max}}$ (Å <sup>-1</sup> )	0.716
Refinement	
$R[F^2 > 2\sigma(F^2)], wR(F^2), S$	0.035, 0.080, 1.01
No. of reflections	4897
No. of parameters	198
H-atom treatment	H atoms treated by a mixture of independent and constrained refinement
$\Delta\rho_{\text{max}}, \Delta\rho_{\text{min}}$ (e Å <sup>-3</sup> )	0.39, -0.25

Computer programs: APEX2 and SAINT (Bruker, 2012), SHELXS97 (Sheldrick, 2008), SHELXL2013 (Sheldrick, 2015), Mercury (Macrae *et al.*, 2006) and PLATON (Spek, 2009).

## References

- Allen, F. H. (2002). *Acta Cryst.* **B58**, 380–388.
- Ashcroft, F. M. (1999). *Ion channels and disease*. New York: Academic Press.
- Ballester, P. (2008). *Recognition of anions*. New York: Springer Science & Business Media.
- Blanchard, L. A., Gu, Z. & Brennecke, J. F. (2001). *J. Phys. Chem. B*, **105**, 2437–2444.
- Bruker (2012). APEX2, SAINT and SADABS. Bruker AXS Inc., Madison, Wisconsin, USA.
- Chauvin, Y. & Olivier-Bourbigou, H. (1995). *Chemtech*, **25**, 26–30.
- Chidan Kumar, C. S., Sim, A. J., Ng, W. Z., Chia, T. S., Loh, W.-S., Kwong, H. C., Quah, C. K., Naveen, S., Lokanath, N. K. & Warad, I. (2017). *Acta Cryst.* **E73**, 927–931.
- Crosthwaite, J. M., Aki, S. N., Maginn, E. J. & Brennecke, J. F. (2004). *J. Phys. Chem. B*, **108**, 5113–5119.
- Davis, J. H. Jr (2004). *Chem. Lett.* **33**, 1072–1077.
- Frontera, A., Gamez, P., Mascal, M., Mooibroek, T. J. & Reedijk, J. (2011). *Angew. Chem.* **123**, 9736–9756.
- Hay, B. P. & Bryantsev, V. S. (2008). *Chem. Commun.* pp. 2417–2428.
- Holbrey, J. & Seddon, K. (1999). *Clean Prod. Process.* **1**, 223–236.
- Lamanna, G., Russier, J., Dumortier, H. & Bianco, A. (2012). *Biomaterials*, **33**, 5610–5617.
- Liu, J., Obando, D., Liao, V., Lifa, T. & Codd, R. (2011). *Eur. J. Med. Chem.* **46**, 1949–1963.
- Macrae, C. F., Edgington, P. R., McCabe, P., Pidcock, E., Shields, G. P., Taylor, R., Towler, M. & van de Streek, J. (2006). *J. Appl. Cryst.* **39**, 453–457.
- Piérard, G. E., Piérard-Franchimont, C., Paquet, P. & Quatresooz, P. (2009). *Expert Opin. Drug Metab. Toxicol.* **5**, 1565–1575.

- Priyanka, B., Anitha, K., Shirisha, S., Dipankar, B. & Rajesh, K. (2013). *Int. Res. J. Pharm. App. Sci.* **3**, 93–101.
- Reisberg, B., Doody, R., Stöffler, A., Schmitt, F., Ferris, S., & Möbius, H. J. (2003). *N. Engl. J. Med.* **348**, 1333–1341.
- Rouchal, M., Nečas, M. & Vícha, R. (2011). *Acta Cryst.* **E67**, o3198.
- Said, M. A., Aouad, M. R., Hughes, D. L., Almeahadi, M. A. & Messali, M. (2017). *Acta Cryst.* **E73**, 1831–1834.
- Schottel, B. L., Chifotides, H. T. & Dunbar, K. R. (2008). *Chem. Soc. Rev.* **37**, 68–83.
- Sharmila, N., Sundar, T. V., Yasodha, A., Puratchikody, A. & Sridhar, B. (2014). *Acta Cryst.* **E70**, o1293–o1294.
- Sheldrick, G. M. (2008). *Acta Cryst.* **A64**, 112–122.
- Sheldrick, G. M. (2015). *Acta Cryst.* **C71**, 3–8.
- Sheshadri, S. N., Kwong, H. C., Chidan Kumar, C. S., Quah, C. K., Siddaraju, B. P., Veeraiah, M. K., Hamid, M. A. B. A. & Warad, I. (2018). *Acta Cryst.* **E74**, 752–756.
- Spackman, M. A. & Jayatilaka, D. (2009). *CrystEngComm*, **11**, 19–32.
- Spackman, M. A. & McKinnon, J. J. (2002). *CrystEngComm*, **4**, 378–392.
- Spackman, M. A., McKinnon, J. J. & Jayatilaka, D. (2008). *CrystEngComm*, **10**, 377–388.
- Spek, A. L. (2009). *Acta Cryst.* **D65**, 148–155.
- Wolff, S. K., Grimwood, D. J., McKinnon, J. J., Turner, M. J., Jayatilaka, D. & Spackman, M. A. (2012). *CrystalExplorer*. University of Western Australia.
- Yue, W. W., Li, H. J., Xiang, T., Qin, H., Sun, S. D. & Zhao, C. S. (2013). *J. Membr. Sci.* **446**, 79–91.
- Zettl, H., Schubert-Zsilavecz, M. & Steinhilber, D. (2010). *Chem-MedChem*, **5**, 179–185.
- Zoidis, G., Kolocouris, N., Kelly, J. M., Prathalingam, S. R., Naesens, L. & De Clercq, E. (2010). *Eur. J. Med. Chem.* **45**, 5022–5030.

## supporting information

*Acta Cryst.* (2018). E74, 1030-1034 [https://doi.org/10.1107/S2056989018009131]

## Crystal structure and Hirshfeld surface analysis of a pyridinium bromide salt: 1-[2-(adamantan-1-yl)-2-oxoethyl]pyridin-4-iminium bromide

Huey Chong Kwong, Imdad Mahmud Pathi, C. S. Chidan Kumar, Ching Kheng Quah and Md. Azharul Arafath

### Computing details

Data collection: *APEX2* (Bruker, 2012); cell refinement: *SAINT* (Bruker, 2012); data reduction: *SAINT* (Bruker, 2012); program(s) used to solve structure: *SHELXS97* (Sheldrick, 2008); program(s) used to refine structure: *SHELXL2013* (Sheldrick, 2015); molecular graphics: *SHELXL2013* (Sheldrick, 2015) and *Mercury* (Macrae *et al.*, 2006); software used to prepare material for publication: *SHELXL2013* (Sheldrick, 2015) and *PLATON* (Spek, 2009).

### 1-[2-(Adamantan-1-yl)-2-oxoethyl]pyridin-4-iminium bromide

#### Crystal data

$C_{17}H_{23}N_2O^+ \cdot Br^-$   
 $M_r = 351.28$   
 Monoclinic,  $P2_1/c$   
 $a = 18.758$  (2) Å  
 $b = 7.1508$  (8) Å  
 $c = 11.9909$  (14) Å  
 $\beta = 98.2117$  (17)°  
 $V = 1591.9$  (3) Å<sup>3</sup>  
 $Z = 4$

$F(000) = 728$   
 $D_x = 1.466$  Mg m<sup>-3</sup>  
 Mo  $K\alpha$  radiation,  $\lambda = 0.71073$  Å  
 Cell parameters from 7278 reflections  
 $\theta = 3.1$ – $25.2$ °  
 $\mu = 2.58$  mm<sup>-1</sup>  
 $T = 294$  K  
 Plate, colourless  
 $0.38 \times 0.25 \times 0.09$  mm

#### Data collection

Bruker APEXII DUO CCD area-detector diffractometer  
 Radiation source: fine-focus sealed tube  
 Graphite monochromator  
 $\varphi$  and  $\omega$  scans  
 Absorption correction: multi-scan (SADABS; Bruker, 2012)  
 $T_{\min} = 0.320$ ,  $T_{\max} = 0.408$

35418 measured reflections  
 4897 independent reflections  
 3392 reflections with  $I > 2\sigma(I)$   
 $R_{\text{int}} = 0.051$   
 $\theta_{\max} = 30.6$ °,  $\theta_{\min} = 2.2$ °  
 $h = -26 \rightarrow 26$   
 $k = -10 \rightarrow 10$   
 $l = -17 \rightarrow 17$

#### Refinement

Refinement on  $F^2$   
 Least-squares matrix: full  
 $R[F^2 > 2\sigma(F^2)] = 0.035$   
 $wR(F^2) = 0.080$   
 $S = 1.01$   
 4897 reflections  
 198 parameters  
 0 restraints

Hydrogen site location: mixed  
 H atoms treated by a mixture of independent and constrained refinement  
 $w = 1/[\sigma^2(F_o^2) + (0.0364P)^2 + 0.3328P]$   
 where  $P = (F_o^2 + 2F_c^2)/3$   
 $(\Delta/\sigma)_{\max} = 0.001$   
 $\Delta\rho_{\max} = 0.39$  e Å<sup>-3</sup>  
 $\Delta\rho_{\min} = -0.25$  e Å<sup>-3</sup>

*Special details*

**Experimental.** The following wavelength and cell were deduced by SADABS from the direction cosines etc. They are given here for emergency use only: CELL 0.71078 12.009 7.162 18.799 89.983 98.202 90.025

**Geometry.** All esds (except the esd in the dihedral angle between two l.s. planes) are estimated using the full covariance matrix. The cell esds are taken into account individually in the estimation of esds in distances, angles and torsion angles; correlations between esds in cell parameters are only used when they are defined by crystal symmetry. An approximate (isotropic) treatment of cell esds is used for estimating esds involving l.s. planes.

*Fractional atomic coordinates and isotropic or equivalent isotropic displacement parameters ( $\text{\AA}^2$ )*

	<i>x</i>	<i>y</i>	<i>z</i>	$U_{\text{iso}}^*/U_{\text{eq}}$
Br1	0.18668 (2)	0.58832 (3)	0.43377 (2)	0.04161 (8)
O1	0.16460 (7)	0.2172 (2)	0.22373 (11)	0.0449 (3)
N1	0.09073 (8)	0.11925 (19)	0.39566 (12)	0.0287 (3)
N2	-0.12926 (9)	0.1691 (3)	0.35275 (16)	0.0399 (4)
H1N2	-0.1522 (14)	0.122 (3)	0.294 (2)	0.060 (8)*
H2N2	-0.1491 (11)	0.232 (3)	0.3994 (18)	0.046 (6)*
C1	0.28202 (10)	0.1231 (3)	0.31057 (14)	0.0334 (4)
C2	0.32236 (11)	0.1050 (4)	0.43067 (16)	0.0487 (6)
H2A	0.3014	0.0049	0.4699	0.058*
H2B	0.3180	0.2204	0.4717	0.058*
C3	0.40229 (11)	0.0632 (4)	0.4260 (2)	0.0617 (7)
H3A	0.4278	0.0525	0.5029	0.074*
C4	0.40873 (13)	-0.1190 (4)	0.3647 (2)	0.0647 (7)
H4A	0.3876	-0.2193	0.4034	0.078*
H4B	0.4591	-0.1483	0.3636	0.078*
C5	0.37011 (12)	-0.1023 (4)	0.2448 (2)	0.0551 (6)
H5A	0.3751	-0.2198	0.2045	0.066*
C6	0.28984 (11)	-0.0621 (3)	0.24763 (17)	0.0433 (5)
H6A	0.2687	-0.1634	0.2855	0.052*
H6B	0.2646	-0.0533	0.1713	0.052*
C7	0.31564 (11)	0.2816 (3)	0.2499 (2)	0.0513 (5)
H7A	0.3111	0.3987	0.2891	0.062*
H7B	0.2906	0.2941	0.1737	0.062*
C8	0.43485 (13)	0.2227 (5)	0.3659 (3)	0.0765 (8)
H8A	0.4306	0.3390	0.4060	0.092*
H8B	0.4856	0.1988	0.3639	0.092*
C9	0.40260 (13)	0.0572 (4)	0.1841 (2)	0.0672 (8)
H9A	0.4531	0.0318	0.1808	0.081*
H9B	0.3779	0.0676	0.1076	0.081*
C10	0.39530 (12)	0.2385 (4)	0.2467 (2)	0.0653 (7)
H10A	0.4166	0.3403	0.2077	0.078*
C11	0.20180 (10)	0.1573 (3)	0.30656 (14)	0.0317 (4)
C12	0.16924 (9)	0.0976 (3)	0.40968 (15)	0.0301 (4)
H12A	0.1813	-0.0324	0.4260	0.036*
H12B	0.1905	0.1715	0.4738	0.036*
C13	0.04945 (10)	0.0291 (3)	0.31040 (15)	0.0357 (4)
H13A	0.0718	-0.0446	0.2616	0.043*

C14	-0.02299 (10)	0.0429 (3)	0.29395 (15)	0.0353 (4)
H14A	-0.0498	-0.0198	0.2341	0.042*
C15	-0.05818 (10)	0.1526 (3)	0.36771 (14)	0.0295 (4)
C16	-0.01401 (9)	0.2433 (2)	0.45605 (14)	0.0300 (4)
H16A	-0.0348	0.3164	0.5069	0.036*
C17	0.05879 (10)	0.2251 (2)	0.46772 (14)	0.0297 (4)
H17A	0.0872	0.2867	0.5264	0.036*

*Atomic displacement parameters (Å<sup>2</sup>)*

	$U^{11}$	$U^{22}$	$U^{33}$	$U^{12}$	$U^{13}$	$U^{23}$
Br1	0.05492 (14)	0.03289 (11)	0.03750 (11)	0.00147 (9)	0.00823 (8)	-0.00127 (8)
O1	0.0371 (8)	0.0609 (10)	0.0352 (7)	0.0074 (7)	0.0001 (6)	0.0094 (7)
N1	0.0278 (8)	0.0256 (8)	0.0330 (7)	-0.0007 (6)	0.0051 (6)	-0.0020 (6)
N2	0.0300 (9)	0.0507 (11)	0.0389 (9)	0.0022 (8)	0.0051 (8)	-0.0078 (8)
C1	0.0276 (9)	0.0426 (11)	0.0295 (8)	-0.0005 (8)	0.0028 (7)	0.0024 (7)
C2	0.0304 (10)	0.0816 (17)	0.0330 (9)	-0.0033 (11)	0.0009 (8)	-0.0015 (10)
C3	0.0273 (11)	0.109 (2)	0.0454 (12)	0.0014 (13)	-0.0049 (9)	0.0035 (13)
C4	0.0344 (12)	0.092 (2)	0.0681 (16)	0.0187 (13)	0.0077 (11)	0.0252 (14)
C5	0.0452 (13)	0.0659 (16)	0.0550 (13)	0.0171 (11)	0.0094 (10)	-0.0039 (11)
C6	0.0355 (11)	0.0506 (13)	0.0427 (10)	0.0056 (9)	0.0018 (8)	-0.0041 (9)
C7	0.0434 (12)	0.0528 (14)	0.0613 (13)	0.0005 (10)	0.0198 (10)	0.0138 (11)
C8	0.0323 (13)	0.102 (2)	0.096 (2)	-0.0162 (14)	0.0110 (13)	-0.0112 (18)
C9	0.0450 (14)	0.105 (2)	0.0562 (14)	0.0200 (14)	0.0234 (11)	0.0144 (14)
C10	0.0453 (14)	0.0729 (18)	0.0839 (18)	-0.0032 (12)	0.0307 (13)	0.0217 (15)
C11	0.0312 (10)	0.0329 (9)	0.0309 (9)	-0.0004 (8)	0.0035 (7)	-0.0012 (7)
C12	0.0248 (9)	0.0298 (9)	0.0357 (8)	0.0041 (7)	0.0042 (7)	0.0028 (7)
C13	0.0352 (10)	0.0347 (10)	0.0380 (9)	-0.0021 (8)	0.0076 (8)	-0.0130 (8)
C14	0.0345 (10)	0.0373 (10)	0.0342 (9)	-0.0045 (8)	0.0052 (8)	-0.0107 (8)
C15	0.0307 (10)	0.0277 (8)	0.0308 (8)	0.0011 (7)	0.0067 (7)	0.0031 (7)
C16	0.0336 (10)	0.0288 (9)	0.0290 (8)	0.0024 (8)	0.0089 (7)	-0.0017 (7)
C17	0.0362 (10)	0.0256 (8)	0.0275 (8)	-0.0022 (7)	0.0053 (7)	-0.0013 (7)

*Geometric parameters (Å, °)*

O1—C11	1.208 (2)	C6—H6A	0.9700
N1—C17	1.352 (2)	C6—H6B	0.9700
N1—C13	1.354 (2)	C7—C10	1.531 (3)
N1—C12	1.466 (2)	C7—H7A	0.9700
N2—C15	1.325 (2)	C7—H7B	0.9700
N2—H1N2	0.85 (3)	C8—C10	1.517 (4)
N2—H2N2	0.84 (2)	C8—H8A	0.9700
C1—C11	1.518 (3)	C8—H8B	0.9700
C1—C7	1.530 (3)	C9—C10	1.514 (4)
C1—C2	1.534 (3)	C9—H9A	0.9700
C1—C6	1.542 (3)	C9—H9B	0.9700
C2—C3	1.538 (3)	C10—H10A	0.9800
C2—H2A	0.9700	C11—C12	1.517 (2)



C2—H2B	0.9700	C12—H12A	0.9700
C3—C4	1.509 (4)	C12—H12B	0.9700
C3—C8	1.523 (4)	C13—C14	1.348 (3)
C3—H3A	0.9800	C13—H13A	0.9300
C4—C5	1.520 (3)	C14—C15	1.414 (2)
C4—H4A	0.9700	C14—H14A	0.9300
C4—H4B	0.9700	C15—C16	1.407 (2)
C5—C9	1.526 (4)	C16—C17	1.359 (2)
C5—C6	1.538 (3)	C16—H16A	0.9300
C5—H5A	0.9800	C17—H17A	0.9300
C17—N1—C13	119.43 (15)	C1—C7—H7B	109.8
C17—N1—C12	121.03 (15)	C10—C7—H7B	109.8
C13—N1—C12	119.53 (15)	H7A—C7—H7B	108.2
C15—N2—H1N2	117.3 (18)	C10—C8—C3	109.1 (2)
C15—N2—H2N2	119.2 (14)	C10—C8—H8A	109.9
H1N2—N2—H2N2	123 (2)	C3—C8—H8A	109.9
C11—C1—C7	109.85 (16)	C10—C8—H8B	109.9
C11—C1—C2	113.40 (15)	C3—C8—H8B	109.9
C7—C1—C2	109.10 (17)	H8A—C8—H8B	108.3
C11—C1—C6	106.61 (15)	C10—C9—C5	109.47 (19)
C7—C1—C6	109.20 (16)	C10—C9—H9A	109.8
C2—C1—C6	108.58 (17)	C5—C9—H9A	109.8
C1—C2—C3	109.56 (16)	C10—C9—H9B	109.8
C1—C2—H2A	109.8	C5—C9—H9B	109.8
C3—C2—H2A	109.8	H9A—C9—H9B	108.2
C1—C2—H2B	109.8	C9—C10—C8	109.7 (2)
C3—C2—H2B	109.8	C9—C10—C7	110.0 (2)
H2A—C2—H2B	108.2	C8—C10—C7	109.8 (2)
C4—C3—C8	110.5 (2)	C9—C10—H10A	109.1
C4—C3—C2	109.4 (2)	C8—C10—H10A	109.1
C8—C3—C2	109.3 (2)	C7—C10—H10A	109.1
C4—C3—H3A	109.2	O1—C11—C12	121.17 (16)
C8—C3—H3A	109.2	O1—C11—C1	122.46 (16)
C2—C3—H3A	109.2	C12—C11—C1	116.20 (15)
C3—C4—C5	109.4 (2)	N1—C12—C11	113.06 (14)
C3—C4—H4A	109.8	N1—C12—H12A	109.0
C5—C4—H4A	109.8	C11—C12—H12A	109.0
C3—C4—H4B	109.8	N1—C12—H12B	109.0
C5—C4—H4B	109.8	C11—C12—H12B	109.0
H4A—C4—H4B	108.2	H12A—C12—H12B	107.8
C4—C5—C9	109.9 (2)	C14—C13—N1	122.10 (16)
C4—C5—C6	109.24 (19)	C14—C13—H13A	119.0
C9—C5—C6	109.26 (19)	N1—C13—H13A	119.0
C4—C5—H5A	109.5	C13—C14—C15	119.97 (17)
C9—C5—H5A	109.5	C13—C14—H14A	120.0
C6—C5—H5A	109.5	C15—C14—H14A	120.0
C5—C6—C1	109.47 (17)	N2—C15—C16	122.28 (17)

C5—C6—H6A	109.8	N2—C15—C14	121.01 (17)
C1—C6—H6A	109.8	C16—C15—C14	116.71 (16)
C5—C6—H6B	109.8	C17—C16—C15	120.57 (16)
C1—C6—H6B	109.8	C17—C16—H16A	119.7
H6A—C6—H6B	108.2	C15—C16—H16A	119.7
C1—C7—C10	109.44 (19)	N1—C17—C16	121.23 (16)
C1—C7—H7A	109.8	N1—C17—H17A	119.4
C10—C7—H7A	109.8	C16—C17—H17A	119.4
C11—C1—C2—C3	177.81 (19)	C3—C8—C10—C7	61.0 (3)
C7—C1—C2—C3	-59.4 (2)	C1—C7—C10—C9	60.2 (2)
C6—C1—C2—C3	59.5 (2)	C1—C7—C10—C8	-60.5 (3)
C1—C2—C3—C4	-60.9 (3)	C7—C1—C11—O1	40.2 (3)
C1—C2—C3—C8	60.3 (3)	C2—C1—C11—O1	162.52 (19)
C8—C3—C4—C5	-59.1 (3)	C6—C1—C11—O1	-78.1 (2)
C2—C3—C4—C5	61.3 (3)	C7—C1—C11—C12	-144.55 (17)
C3—C4—C5—C9	58.7 (2)	C2—C1—C11—C12	-22.2 (2)
C3—C4—C5—C6	-61.2 (3)	C6—C1—C11—C12	97.25 (18)
C4—C5—C6—C1	60.4 (2)	C17—N1—C12—C11	-122.92 (17)
C9—C5—C6—C1	-59.9 (2)	C13—N1—C12—C11	58.3 (2)
C11—C1—C6—C5	178.04 (16)	O1—C11—C12—N1	0.6 (3)
C7—C1—C6—C5	59.4 (2)	C1—C11—C12—N1	-174.80 (15)
C2—C1—C6—C5	-59.5 (2)	C17—N1—C13—C14	0.7 (3)
C11—C1—C7—C10	-175.80 (19)	C12—N1—C13—C14	179.53 (17)
C2—C1—C7—C10	59.3 (2)	N1—C13—C14—C15	-0.6 (3)
C6—C1—C7—C10	-59.2 (2)	C13—C14—C15—N2	179.56 (19)
C4—C3—C8—C10	59.7 (3)	C13—C14—C15—C16	0.1 (3)
C2—C3—C8—C10	-60.7 (3)	N2—C15—C16—C17	-179.07 (18)
C4—C5—C9—C10	-59.4 (3)	C14—C15—C16—C17	0.4 (3)
C6—C5—C9—C10	60.4 (3)	C13—N1—C17—C16	-0.2 (3)
C5—C9—C10—C8	60.2 (3)	C12—N1—C17—C16	-179.00 (16)
C5—C9—C10—C7	-60.7 (3)	C15—C16—C17—N1	-0.4 (3)
C3—C8—C10—C9	-59.9 (3)		

### Hydrogen-bond geometry ( $\text{\AA}$ , $^\circ$ )

Cg1 is the centroid of the N1/C13–C17 ring.

$D-H\cdots A$	$D-H$	$H\cdots A$	$D\cdots A$	$D-H\cdots A$
N2—H1N2 $\cdots$ Br1 <sup>i</sup>	0.84 (2)	2.73 (2)	3.499 (2)	153 (2)
N2—H2N2 $\cdots$ Br1 <sup>ii</sup>	0.85 (2)	2.56 (2)	3.393 (2)	169 (2)
C12—H12A $\cdots$ Br1 <sup>iii</sup>	0.97	2.72	3.664 (2)	166
C17—H17A $\cdots$ O1 <sup>iv</sup>	0.93	2.59	3.434 (2)	150
C14—H14A $\cdots$ Cg1 <sup>i</sup>	0.93	2.94	3.608 (2)	130

Symmetry codes: (i)  $-x, y-1/2, -z+1/2$ ; (ii)  $-x, -y+1, -z+1$ ; (iii)  $x, y-1, z$ ; (iv)  $x, -y+1/2, z+1/2$ .